JOURNAL OF GEOPHYSICAL RESEARCH, VOL. 101, NO. C5, PAGES 12,057–12,069, MAY 15, 1996

Efficiency of mixing in the main thermocline

J. N. Moum

College of Oceanic and Atmospheric Sciences, Oregon State University, Corvallis

Abstract. Estimates of heat flux from direct measurements of vertical velocity–temperature fluctuation correlations have been obtained from vertical profiles through turbulent patches in the main thermocline. These have been compared to more indirect flux estimates derived from dissipation rates of turbulent kinetic energy and temperature variance. Because record lengths are limited by the thickness of observed turbulent patches, uncertainties are larger than would be expected from relatively longer horizontal records. The best estimate of dissipation flux coefficient from these data is about 0.15–0.2, but it is characterized by a large range of sample values. This implies mixing efficiencies (flux Richardson numbers) are about 0.13–0.17. This is within the range of laboratory estimates but is different from measurements in turbulent tidal fronts.

1. Introduction

One of the principal motivations for obtaining measurements of turbulence (or in oceanographers' terms, microstructure) in the ocean has been to quantify the irreversible transports of heat, salt, density, and momentum associated with turbulent mixing. Because direct measurements of fluxes have proven difficult to make and perhaps even more difficult to interpret, the great bulk of our knowledge is based on indirect methods of estimating fluxes. These methods are based on two models, one proposed by *Osborn and Cox* [1972] and one by *Osborn* [1980]. They employ measurements of the dissipation rates of turbulent kinetic energy (TKE) ϵ and of temperature variance χ.

The turbulent flux of heat F (as it appears in the Reynolds-averaged equations) [e.g., *Gregg*, 1987] is given by

$$F \equiv \overline{w'T'}, \tag{1}$$

where w' represents the vertical velocity fluctuation on scales of three-dimensional turbulence and T' is the corresponding temperature fluctuation. For simplicity, the kinematic unit of Kelvin meter per second is used here. Multiplication by ρC_p (where ρ is the density of seawater and C_p is its specific heat) yields the dynamic unit of Watt per square meter. With the standard convention ($z > 0$, upward), $F < 0$ represents upward transport of cool fluid or downward transport of warm fluid signifying downgradient heat transport. Following the notation used by *Gargett and Moum* [1995] (hereinafter referred to as GM95), the two indirect estimates are

$$\Gamma_o F_\epsilon \equiv \Gamma_o \epsilon \frac{T_z}{N^2}, \tag{2}$$

$$F_\chi \equiv \frac{\chi}{2T_z}. \tag{3}$$

The temperature gradient is T_z and $N^2 = -g\rho_o^{-1}\rho_z$ is the buoyancy frequency. Γ_o is intended to be a constant of proportionality, equal to $R_f/(1 - R_f)$, where R_f is a flux Richardson number defined by $R_f = b/s$, b is the buoyancy production of TKE, $b = -g\rho_o^{-1}\overline{w'\rho'}$, and s is the shear production of turbulence. In a stratified turbulent flow, b represents the rate at which potential energy is gained by the fluid system due to turbulence generated at a rate given by s. This implies $\Gamma_o = b/\epsilon$. The working definition of Γ_o (and in GM95) is

$$\Gamma_o = F/F_\epsilon, \tag{4}$$

An approximation to this, derived from (2) and (3), is

$$\Gamma_d = F_\chi/F_\epsilon. \tag{5}$$

Within the framework of these assumptions, R_f is a mixing efficiency. The parameters, Γ_o, Γ_d, are simply related to R_f, but they are not mixing efficiencies. Unfortunately, in our community, we have been referring to Γ_o and Γ_d as mixing efficiencies. I have been unable to find an equivalent thermodynamic term to describe the ratio of potential energy gained by the system to the energy dissipated (this ratio is Γ). For now, I suggest we simply refer to Γ as the dissipation flux coefficient.

Oceanic observations of Γ_d indicate a range of 0.1 to 0.4 [*Moum*, 1990a]. Oceanic observations of Γ_o range from 0.05 from towed measurements at open ocean locations [*Yamazaki and Osborn*, 1993] (hereinafter referred to as YO93) (also see *Fleury and Lueck* [1994] (hereinafter referred to as FL94)) to 0.7 ($F > 0$) and -1 ($F < 0$) from measurements made in a turbulent tidal front by GM95. Laboratory estimates of Γ_o indicate

Paper number 96JC00508.
0148-0227/96/96JC-00508$09.00

values of 0.2 [*Rohr and Van Atta*, 1987] and 0.05 [*Huq and Britter*, 1995].

The definition of the overbar in (1) is critical. The indirect fluxes (2), (3) were derived from the full balance equations for TKE and temperature variance [e.g., *Moum*, 1990a]. The requirements include stationarity and negligible divergence terms. To neglect divergence terms strictly requires averaging over the full three-dimensional volume of the turbulent patch, defined to have no flux through the volume's surface. As this averaging is impossible to achieve from field measurements, the deficiencies in practical definitions of the overbar limit our ability to achieve the appropriate balances. The consequent incomplete resolution of intermittency in the observed turbulence is the single biggest factor contributing to the uncertainty in flux estimates.

Winters et al. [1995, p. 127] remark that "buoyancy flux is an indirect rather than a direct measure of diapycnal mixing." This is certainly true. Mixing occurs by molecular diffusion at the smallest scales where concentration gradients are large. As it is defined in (1), F represents the turbulent stirring of fluid parcels by which local concentration gradients are enhanced, thereby enhancing diffusive mixing. F is referred to here (and elsewhere) as a direct flux estimate because it appears directly in the equations governing TKE and temperature variance. The estimates (2), (3) are derived by equating other measurable quantities (ϵ, χ) in these equations to F. Since this requires us to neglect most of the terms in the equations, the estimates F_ϵ, F_χ are more indirect than F, and these are referred to as indirect flux estimates. Although recent convention is followed here, primarily to avoid confusion with GM95, probably a better term for F (used by our atmospheric colleagues) is eddy-correlation, or covariance, flux.

The objective of this paper is to describe field measurements of F from vertical profiles through the main thermocline and to determine the mixing efficiency associated with stratified turbulence in this regime. The perspective of the measurements is discussed in section 2, followed by a critical assessment of the direct heat flux estimates, including uncertainty estimates, in section 3. Flux comparisons and mixing efficiency estimates are presented in section 4 and discussed in section 5. This is followed by conclusions (section 6).

2. Examples of Turbulent Patches From the Viewpoint of a Vertical Profiler

The data were obtained in the spring of 1991, 1000 km off the coast of northern California. The particulars are discussed in more detail by *Moum* [1996] and *Hebert and Moum* [1994]. All measurements were made from sensors mounted on the vertical microstructure profiler, Chameleon [*Moum et al.*, 1995]. These include temperature, conductivity, horizontal velocity fluctuations (using airfoil probes), and vertical velocity fluctuations (using a pitot tube).

It is a characteristic of vertical records of turbulent patches in the ocean's thermocline that very few and short stretches of the records exhibit turbulence that is sufficiently energetic to be detected by existing measurement systems [e.g., *Gregg*, 1987]. For the purpose of assessing flux calculations and for comparisons of turbulence quantities, it is unreasonable to include data with no detectable signal together with data representing the energetic parts of the record. Consequently, this analysis focuses on the energetic parts of the records or the clearly turbulent patches within the thermocline. Determining the net flux through the thermocline is another matter, requiring an evaluation of the importance of the energetic portions of the thermocline relative to that of the majority of the data, which is below detection limits of current instrumentation. A rationale for data selection follows.

A total of 272 turbulent patches were selected from the upper part of the main thermocline. To be selected, each patch had to have the following: (1) background stratification stably stratified in temperature (which avoids ambiguities in the designation of temperature fluctuation as the difference between in situ and monotonically reordered temperature (discussed in section 3); the problems associated with defining a background stratification are discussed below); (2) measurable signal in all fluctuation quantities; and (3) well-defined upper and lower boundaries between the fluid actively mixing in the patch and the relatively quiescent fluid above and below (which requires $L_t^{\max} < L_p$, where $L_t^{\max}$ denotes the maximum value of the Thorpe scale L_t [*Thorpe*, 1977] throughout the patch and L_p is the thickness of the patch; this also requires that $\int L_t(z)dz$ over L_p is equal to 0).

For each patch, salinity and density were determined from temperature and conductivity. The temperature variance dissipation rate χ was determined from temperature gradient fluctuations. Because the thermistor does not fully resolve the spectrum of temperature gradient variance, a correction was applied based on the Batchelor form of the scalar variance spectrum. The TKE dissipation rate ϵ was determined from horizontal velocity gradient fluctuations. Details of these computations are discussed by *Moum et al.* [1995] and GM95. Vertical velocity fluctuations were determined from pitot tube measurements [*Moum*, 1990b].

Examples of patches are shown in Figures 1a–1c. Patch-averaged or patch root-mean-square (rms) values of important quantities for each patch depicted in Figures 1a–1c are listed in Table 1. In the remainder of the text, fluctuation quantities (those with near-zero mean values through the patch) are generally presented as rms values. These are L_t, T, w; further reference to these unprimed quantities imply that they are rms values. The flux, $w'T'$, is computed as the mean value, as this is how it appears in the equations for turbulent kinetic energy and temperature variance and in (1). These particular examples illustrate the diversity of the kinematic snapshots obtained of turbulent patches

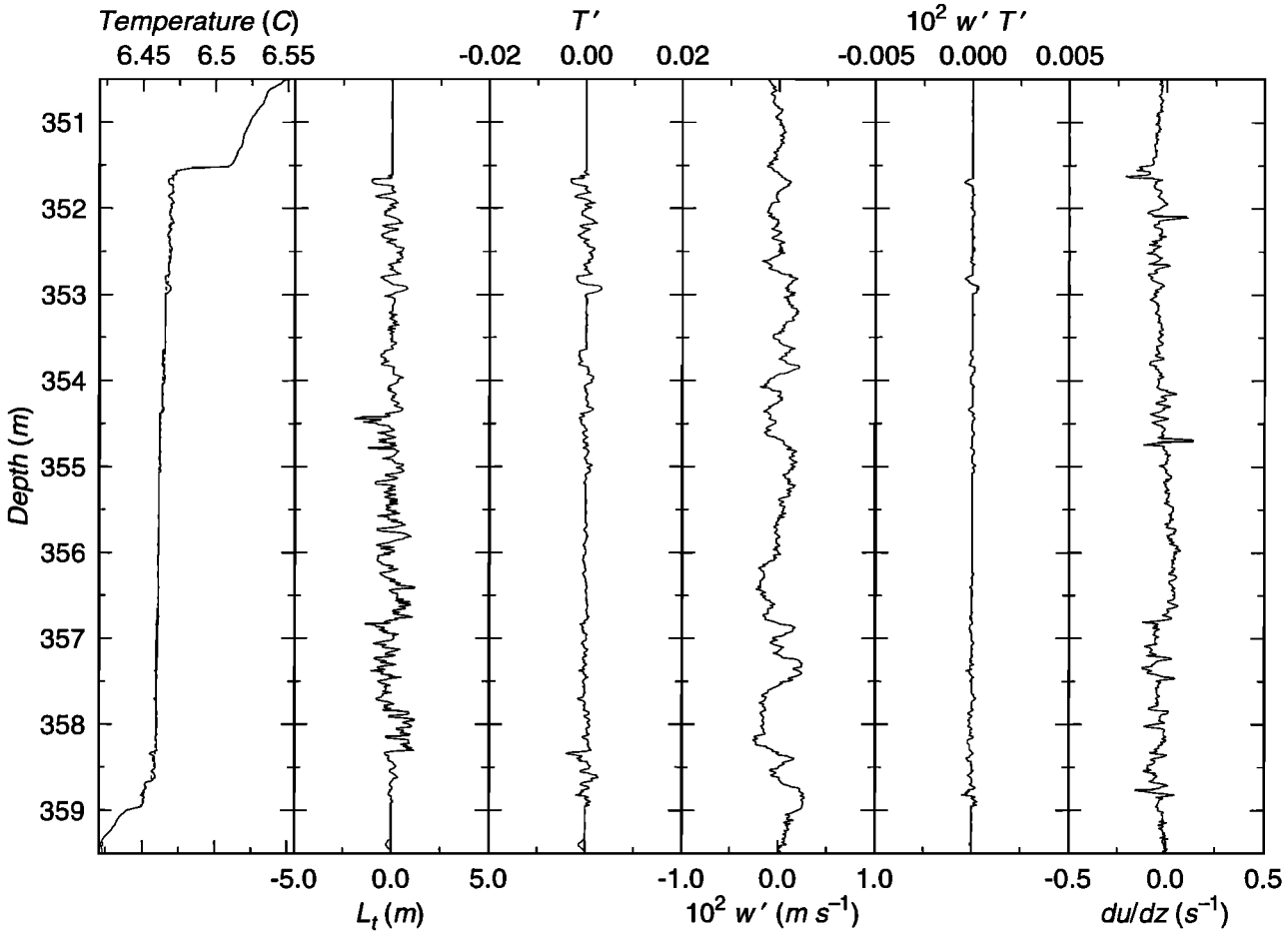

Figure 1a. Example profile through turbulent patches in the upper part of the main thermocline 1000 km off northern California. (from left to right) Observed temperature (solid line) and reordered temperature (dashed line); Thorpe scale L_t; fluctuation temperature, defined as the difference between observed and reordered temperatures; vertical velocity fluctuations w'; $w'T'$, the product of the signals in the third and fourth panels; and horizontal velocity gradient fluctuations, as determined from shear probes. Some patch-averaged values are listed in Table 1.

from vertical profiles. The buoyancy Reynolds numbers, $\epsilon/\nu N^2$, listed in Table 1 indicate that the turbulence is sufficiently intense to excite a broad range of wavenumbers, and we should expect isotropic turbulence at small scales.

Figure 1a portrays a turbulent patch that is relatively uniform in temperature between well-defined upper and lower steps. L_t is also relatively uniform throughout and is approximately equal to L_o, the Ozmidov scale ($L_o = (\epsilon/N^3)^{1/2}$), in agreement with statistical analyses over many patches (*Dillon* [1982]; *Moum* [1995]; and others]. The averaged heat flux F is downgradient.

In contrast, the patch in Figure 1b is steppy. There is considerably more variability in L_t, and the averaged heat flux is countergradient. In instances such as these there arises some ambiguity about the patch selection process. There are five distinct steps between 491 and 504.5 m, defining four layers characterized by local transport within; that is, at the time of the profile, L_t indicates that reordered fluid parcels do not cross steps or $\int L_t(z)dz = 0$ within each step. Is this a single patch or four distinct turbulent patches? For this analysis this example and others like it were designated as single patches. The working hypothesis, in this case, is that although at this time and place, there is no fluid communicating across distinctly defined steps, the full vertical extent is actively turbulent and this particular state represents one of those possible through the evolution of the feature.

A very different example is shown in Figure 1c. In this case there appears to be active overturning from top to bottom over the full vertical extent of the patch. L_t indicates that fluid at the top of the patch is reordered all the way to the bottom and vice versa. Higher-frequency fluctuations in the temperature profile indicate active turbulence at smaller scales as well ($\overline{\epsilon}$ is comparable to those found for the examples shown in Figures 1a and 1b). The downgradient flux is 10–100 times larger than for the patches shown in Figures 1a and 1b, and L_t is considerably larger than L_o.

The definitions (2), (3) for F_ϵ, F_χ require estimates of gradients of T and ρ. These estimates should represent the background stratification against which the TKE is working. The presence of turbulence indicates that the

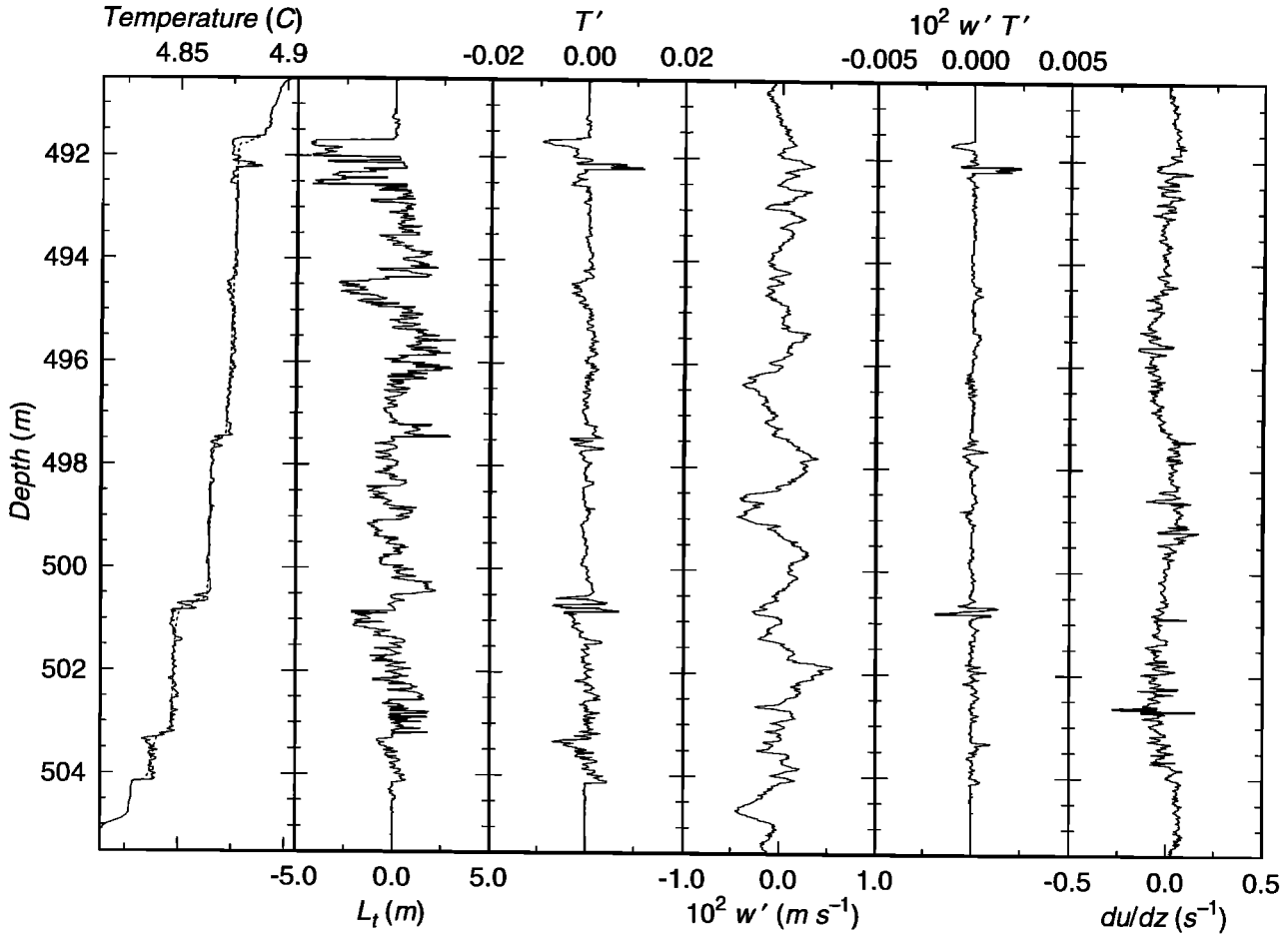

Figure 1b. Same as Figure 1a, but for a different profile.

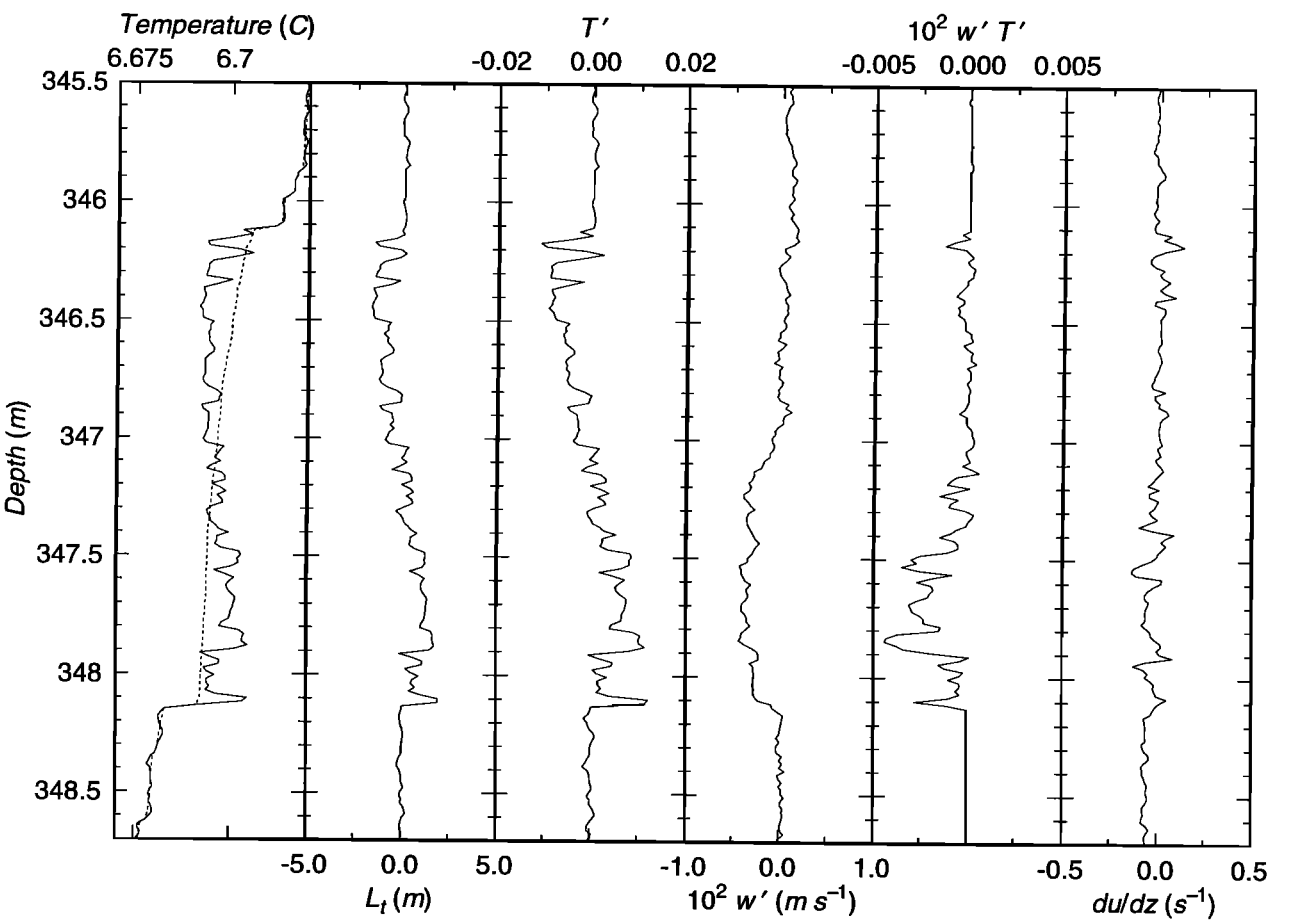

Figure 1c. Same as Figure 1a, but for a different profile.

Table 1. Patch-Averaged Values Determined for the Example Profiles in Figures 1a–1c

	Figure		
Profile	1a	1b	1c
L_t, m	0.48	1.2	0.93
L_o, m	0.96	0.73	0.37
10^3T, K	0.78	1.8	5.3
10^3w, m s^{-1}	1.1	1.7	1.8
10^6F, K m s^{-1}	-0.12	0.31	-7.2
ρC_pF, W m^{-2}	-0.48	1.2	-29
$10^8\epsilon$, m^2 s^{-3}	0.60	0.92	1.2
10^6N^2, s^{-2}	3.5	20	6.7
$\frac{\epsilon}{\nu N^2}$	1700	590	1400

Thorpe scale L_t, temperature T, and vertical velocity w are presented as rms values. The averaged heat flux is shown in both kinematic (Kelvin meter per second) and dynamic unit (Watt per square meter). The density ρ is $\approx$ 1023 kg m^{-3}, and specific heat of seawater C_p is $\approx$ 4000 J kg^{-1} K^{-1}. L_o is Ozmidov scale, F is heat flux, ϵ is turbulent kinetic energy dissipation rate, and N^2 is the buoyancy frequency.

fluid has been stirred and that irreversible mixing may have already occurred. As a consequence, the profiles of T and ρ have been altered from their original profiles that existed before the occurrence of the turbulence. If irreversible mixing has occurred, the original profiles cannot be recovered from the available data. They can only be approximated. *Hebert et al.* [1992] discussed this quandary with a simple example. The density gradient determined from a reordered profile and confined to the limits of the patch boundaries was considered a lower bound on the preexisting density gradient. Any other estimate required determining density differences at depths some small distance above and below the patch and gave larger estimates of gradients. The upper bound estimate was 2.5 times larger than the lower bound. However, the choice of depth interval is arbitrary, and for this analysis, the lower bound estimate is used. If ρ is solely determined by T, this is of no consequence to computations of F_ϵ and Γ_o. However, if T_z is an underestimate, F_χ and Γ_d will be biased high. For this analysis all of the estimates of T_z, ρ_z, and N^2 have been made from the reordered profiles and are intended to be representative of the background, rather than the instantaneous, stratification. As noted by *Peters et al.* [1995], the inability to make a clear determination of the background gradients contributes to scatter in statistical comparisons of quantities that include background gradients.

3. Direct Heat Flux Measurements

3.1. Calculation of w, T

The measurement of w was made using a pitot tube on Chameleon's nose [*Moum*, 1990b]. This sensor resolves 1 mm s^{-1} differences in vertical velocity [*Moum*, 1996]. Of particular concern for this experiment was the filtering effect of the profiler on the measurements of w. The profiler acts as a high-pass filter to scales larger than its vertical dimension. A significant portion of the signal at scales larger than the profiler's length may be lost because the profiler itself responds to those signals, thereby changing the reference frame of the sensors. At large scales the sensors mounted on the profiler cannot, in turn, sense the signal of interest. The shape of the high-pass filter can only be determined empirically and requires additional measurements. A three-axis accelerometer package was in place on Chameleon for this experiment (the configuration was the same as that described by *Moum et al.* [1995] for the Tropical Instability Wave Experiment). No detectable signal due clearly to any source other than vehicle tilt or to operator error was observed, thereby precluding a clean assessment of vehicle response. However, this also indicates that a reasonably small signal is involved.

To minimize the effect of vehicle filtering on the measurements analyzed here, three courses of action were taken. First, the length of the profiler was extended to 4.2 m (a schematic is shown by *Moum et al.* [1995]). The separation between sensors and drag elements was slightly greater than 4 m. Consequently, we expect minimal high-pass filtering of scales smaller than about 4 m. Second, the analysis was restricted to turbulent patches with length scales ℓ < 3 m (as characterized by any of the observationally derived length scales analyzed by *Moum* [1996]; the vast majority were < 1 m). Since the stratification attenuates vertical motion on scales > ℓ, the expectation is that the profiler's high-pass filter does not affect the scales of interest. A consequence of the filtering provided by the measurement platform is that, for any particular patch, the mean value of w is nearly zero. Finally, to further ensure the complete removal of inadequately resolved low-frequency motion, a symmetric high-pass filter of length equivalent to 3.75 m was run over the w data.

A fixed scale separation is introduced by this procedure. It is possible that, in some cases, some vertical motion at scales > 3.75 m has been excluded from the analysis that we should properly consider to be part of the turbulence. It is also possible that we have included some vertical motion at scales < 3.75 m that should be considered part of the internal gravity wave field, or more likely, part of the ill-defined range of scales bounded by waves and fully developed turbulence. The rationale for the selection of patches was intended to minimize this cross talk of scales.

While the definition of fluctuation vertical velocity is relatively straightforward, that for fluctuation temperature is less so. Usually, for horizontal flux measurements made in the atmosphere [*Fairall et al.*, 1990] or in the ocean (GM95) the same filter is applied both to w and to T, so that each represents the same signal bandwidth. However, high-pass filtering of the temperature signal in the vertical coordinate direction can produce spurious results due to the sharpness of mean vertical temperature gradients, especially at the edges of turbulent patches (Figure 1). A better definition is the

deviation of the observed temperature profile from that profile reordered to represent the lowest potential energy state achievable using the observed data; this is the Thorpe-reordered profile [*Thorpe*, 1977]. This provides a clear separation between instantaneous and reordered (or background) states. Insofar as this distinguishes between turbulence and the background state of the flow field, it also provides a clear scale separation. From a three-dimensional reordering procedure (as might be achieved using output from numerical simulations) this definition requires the mean value of T' over the turbulent patch to be 0. *Winters et al.* [1995] have constructed such a numerical framework and demonstrated that this definition of T' (ρ' in their computations) is appropriate when computed from a fully resolved three-dimensional field. The one-dimensional analogue dictated by oceanic field measurements cannot fully resolve the fluctuations, and there will be a contribution from unresolved lateral advection of fluid parcels within the patch. However, several indicators suggest that it is consistent with other measures of stratified turbulence. *Dillon* [1982] demonstrated the correspondence of L_t and L_o (as have others since). He also showed the correspondence between $N\overline{T'^2}$ (using an identical definition of T') and χ. *Moum* [1996] demonstrated similar correspondences from the data discussed here. *Peters et al.* [1995] have recently used this working definition of T' to define a turbulent temperature fluctuation scale.

3.2. Significance

To test whether an individual estimate of F is significantly different from zero, the w' and T' series from a single record were randomly resampled, combined as $w'T'$, and averaged over the same number of points as in the original record. The correlation coefficient between w' and T', $r_{wT} = F/[w_{\rm rms} \times T_{\rm rms}]$, was computed for each estimate of F. This was done 500 times and the 95% confidence limits computed as the middle 95% range of all 500 randomly sampled r_{wT} estimates. This procedure is somewhat different from that followed by GM95, YO93, and FL94, in which random lags were applied that exceeded the autocorrelation times of w' and T' signals. Because of the relatively short data records available from the vertical profile data, such an approach proved unreasonable here. As pointed out by one reviewer, this may serve to bias the correlation coefficients to lower values. For an estimate to be considered significant it had to lie outside the 95% confidence limits of the randomly constructed estimates of $\overline{w'T'}$. This sorting of the data reduced the number of records for further analysis from 272 to 110.

3.3. Spectra

Spectra of the fluctuation quantities w', T', were computed for each of the 110 patches analyzed. Time series of 256 points were windowed and overlapped to fit within patch boundaries. The number of 256-point series in each patch varied with the patch thicknesses. Since individual record lengths were relatively short, spectra were determined for each patch, normalized for that patch, and then ensemble-averaged over many patches. These include both positive and negative F values. The following two normalizations were used.

1. For the spectra shown in Figure 2, temperature spectra were nondimensionalized by the Batchelor form ($\phi_B = \chi\epsilon^{-1/3}k_B^{-5/3}$, where $k_B = (\epsilon/(\nu D^2))^{1/4}$ is the Batchelor wavenumber, ν is the kinematic viscosity, and D is the molecular diffusivity for temperature in water). Frequencies were nondimensionalized by the Batchelor frequency, $f_B = Uk_B/2\pi$, where U, the speed at which the probe traverses the turbulence, is represented by the vehicle's fall speed. Vertical velocity spectra were nondimensionalized by the Kolmogoroff form ($\phi_s = (\epsilon\nu^5)^{1/4}$), and the associated frequencies by the Kolmogoroff frequency, $f_s = Uk_s/2\pi$, where $k_s = (\epsilon/(\nu^3))^{1/4}$.

2. To emphasize the dominant scales, spectra were normalized by their variance and then ensemble averaged (Figure 3). While the series are sampled as time series, conversion to spatial series (from which the top scale in Figure 3 is derived) was approximated using the mean fall speed of the profiler (≈ 0.75 m s^{-1}). Displayed in variance-preserving form, the spectra show clear peaks. The equivalent length scale at the peak in

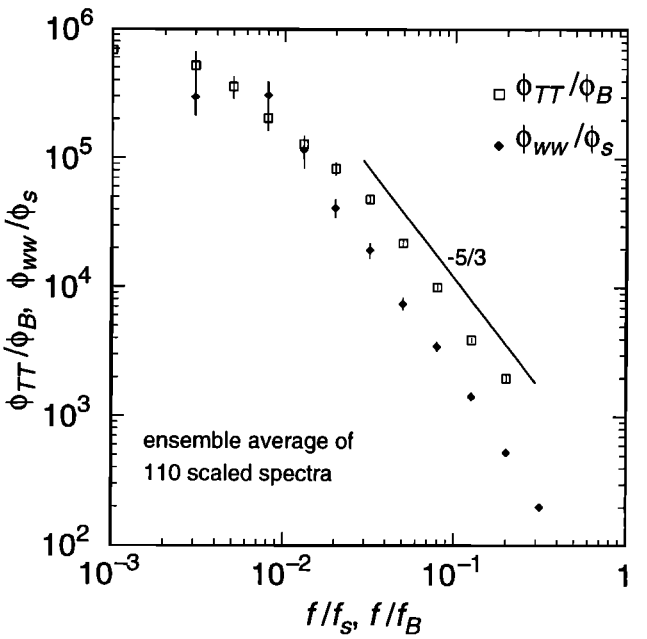

Figure 2. Nondimensionalized spectra of w', T'. Raw spectra were computed for each of 110 patches examined, nondimensionalized by Kolmogoroff scaling (for w' spectra) or Batchelor scaling (for T' spectra), and ensemble averaged over all patches. Only those patches for which the correlation coefficient between w' and T' is significant were averaged. (Note that remaining figures depict data from only these records.)

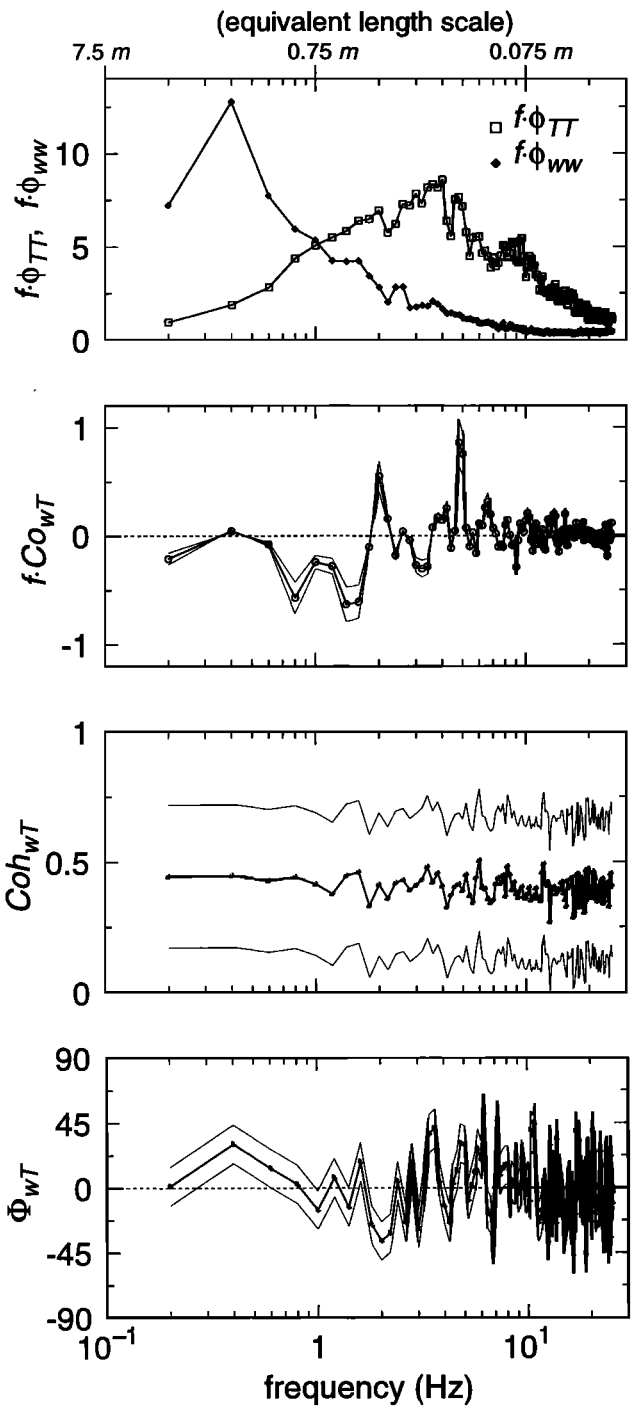

Figure 3. Ensemble-averaged spectra of w' (ϕ_{ww}), T' (ϕ_{TT}) and cospectra of $w'T'$ (Co_{wT}), nondimensionalized by their variance and presented in variance-preserving form. Also shown are coincident, ensemble-averaged squared coherence (Coh_{wT}) and phase (Φ_{wT}) spectra.

the T' spectrum is about 0.2 m, while that of the w' spectrum is about 2 m.

Flux cospectra (i.e., cospectra of $w'T'$) were computed for the records analyzed above, normalized by the variance or flux, ensemble-averaged, and displayed in variance-preserving form (Figure 3). The averaged cospectrum (again, including both positive and negative F values) is clearly dominated by downgradient (< 0) features with scales of about 0.5–1 m. For completeness, squared coherence and phase spectra are also shown. The small values of the phase spectrum at all frequencies indicates the minimal role of the quadrature part of the cross spectrum (which would include internal gravity waves) in these data. This is an indicator of high Re turbulence.

Several characteristics of the spectra shown in Figure 3 are qualitatively different from their horizontally derived equivalents obtained in both the atmospheric boundary layer [e.g., *Kaimal et al.*, 1972; *Pond et al.*, 1971] and the tidal front (GM95). The thermocline data show no k^{-1} region at low wavenumbers, present in the atmospheric boundary layer and tidal front data. While the atmospheric boundary layer and tidal front results indicate a spectral peak in T' at a wavenumber less than the wavenumber of the spectral peak of w', the opposite is true for these thermocline data. The flux cospectrum peaks at a wavenumber/frequency between those of peaks in T' and w' spectra.

The ensemble-averaged spectrum of vertical velocity is attenuated at the lowest frequency bin, which is equivalent to a length scale of 3.75 m (given a constant vehicle fall rate of 0.75 m s^{-1}). This is the length of the digital high-pass filter applied to ensure the complete removal of any w' signal that is inadequately resolved by the measurement. Apparently, any signal removed by the filter contains minimal contributions to the turbulence. If it did, the scale relation demonstrated by *Moum* [1996] using these same data and processing methods to represent an inviscid estimate of ϵ ($\approx Nw^2$) over nearly four decades of domain space would not be so consistent over the full range of observed values.

Does the attenuation of w' at low frequencies have significant influence on the flux estimates? Individual cospectra, computed from single patches, are highly variable, and occasionally dominated by the signal at the lowest-frequency bin. This is to be expected from random samples of a turbulent flow field. The only way we can begin to examine the behavior of the cospectrum is by averaging. The ensemble-averaged cospectrum indicates a peak at scales substantially smaller than 3.75 m, suggesting that the flux-carrying scales are resolved.

The difference in relative wavenumbers of the peak in the T' spectrum probably reflects the differences in definitions of T' between that used for horizontal measurements and that used here for the vertical profile data. While there are no clear guidelines on how to estimate T' from single profiles (either horizontal or vertical) in a three-dimensional turbulent field, it seems that the definition used here is more tenable and has some theoretical basis [*Winters et al.*, 1995]. That used for horizontal measurements is usually the demeaned signal over the record; this may include gravity waves and other phenomena which are indistinguishable from the turbulent signal because the flow field is underresolved

by the observations. The result of such an analysis will be a larger signal at low wavenumbers.

3.4. Uncertainties

For further statistical comparison, each single patch estimate of F was determined from the arithmetic mean value of $w'T'$ over the turbulent patch. This defines the overbar in (1). The uncertainty in a single estimate is due to a combination of measurement uncertainty and the ability of the measurement to resolve the natural variability or intermittency of the signal. The measurement uncertainty includes both random and systematic contributions and may be written as

$$\frac{\delta F}{F} = \frac{\delta w'}{w'} + \frac{\delta T'}{T'}, \quad (6)$$

where δF refers to the uncertainty in F (and similarly for w' and T'). The systematic contribution is largely due to calibration uncertainties, which are small relative to other sources of uncertainty. The more important contribution is the random uncertainty due to the limited resolution of both signals. The smallest detectable increment in w' is about 0.001 m s^{-1} and in T' is about 0.0005 K. If we consider these to be the uncertainties in each signal, then for relatively small signal levels of $w' =$ 0.005 m s^{-1} and $T' = 0.005$ K, the relative uncertainty in F is 30%.

The most serious problem is associated with the uncertainty due to insufficient sampling. One estimate of the uncertainty can be made in light of analyses made for flux measurements from the atmospheric boundary layer. *Lenschow et al.* [1994] considered stationary time series while acknowledging that real time series are very often far from stationary. They developed expressions for the relative bias [*Lenschow et al.*, 1994, equation (30)] and systematic errors (their equation (48)) in flux estimates due to limited sample durations of processes representative of turbulence in the atmospheric boundary layer. These expressions depend on the record length TI and the integral timescale of the flux correlation function τ_f. The specific problem addressed by *Lenschow et al.* [1994] was to determine how large TI should be to estimate F with a specified statistical uncertainty. In the vertical data examined here there is no clear objective choice for TI, other than to make it unreasonably short; it depends solely on the patch thickness. Following GM95, τ_f is estimated from the peak frequency of the variance-preserving flux cospectrum. This corresponds to a length scale of about 0.5 m. As the patch thicknesses vary from about 1 to 15 m [*Moum*, 1996], the ratio TI/τ_f varies from 2 to 30. The associated bias error is 50% for thin patches and 6% for thick patches.

Lenschow et al.'s [1994] expression for systematic uncertainty includes a dependence on the correlation coefficient r_{wT} between w' and T'. The median value for all of the patches with r_{wT} significantly different from zero is -0.1 (the negative value indicates downgradient flux). The associated systematic uncertainty is a factor of 10 for a 1-m-thick patch, approaching a value of about a factor of 3 for patches of thickness greater than 10 m. For the data considered here, then, we can expect the uncertainty to be no better than a factor of 3 based on this particular formulation.

Another estimate of the uncertainty in the flux estimate was made for each patch estimate of F. The number of degrees of freedom (d.f.) was estimated for each record as the (number of zero crossings of w)/2. As the number of zero crossings of w is considerably less than that of $w'T'$ for any given record (frequently by a factor of 10), this represents a lower bound on d.f. The 95% confidence interval was estimated based on normal statistics as $1.96 \cdot \sigma_{wT}/\text{d.f.}^{1/2}$, where σ_{wT} is the record's standard deviation of $w'T'$. The distribution of the ratio of the confidence interval (CI) defined in this way to the record estimate of F is shown in Figure 4. This indicates 10% of the estimates of CI to be more than $10 \times F$. On the other hand, 50% of the estimates are less than $3 \times F$, which is close to the lower bound on the estimates based on the expressions of *Lenschow et al.* [1994]. This estimate is used in Figure 5 to portray the uncertainty in single-patch estimates.

These estimates of uncertainty are conservative and large. The reason they are large is primarily due to the fact that the samples represent relatively short records in an intermittent field. Hence there are few degrees of freedom in independent estimates of F. This is just a fact of life in dealing with this type of measurement. Increasing the record length requires thicker turbulent patches, a factor over which the investigator has no control. Alternatively, investigations could be contin-

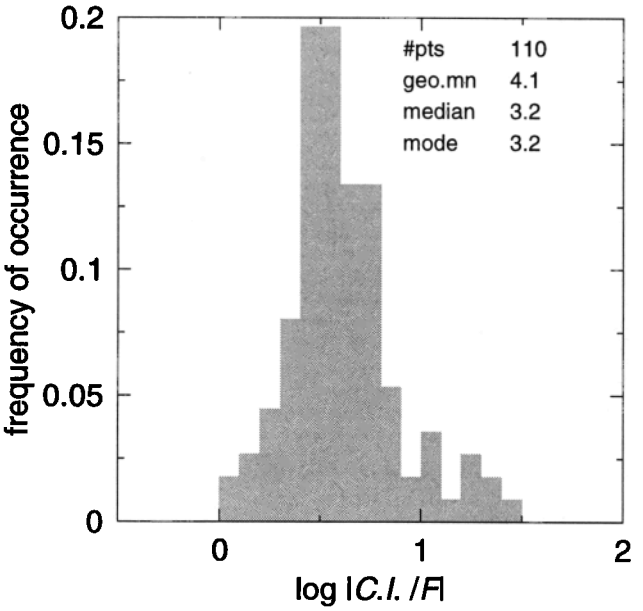

Figure 4. Histogram of the logarithm of the ratio of uncertainty to mean estimate of F. The geometric mean of the ratio and other measures of central tendency are shown.

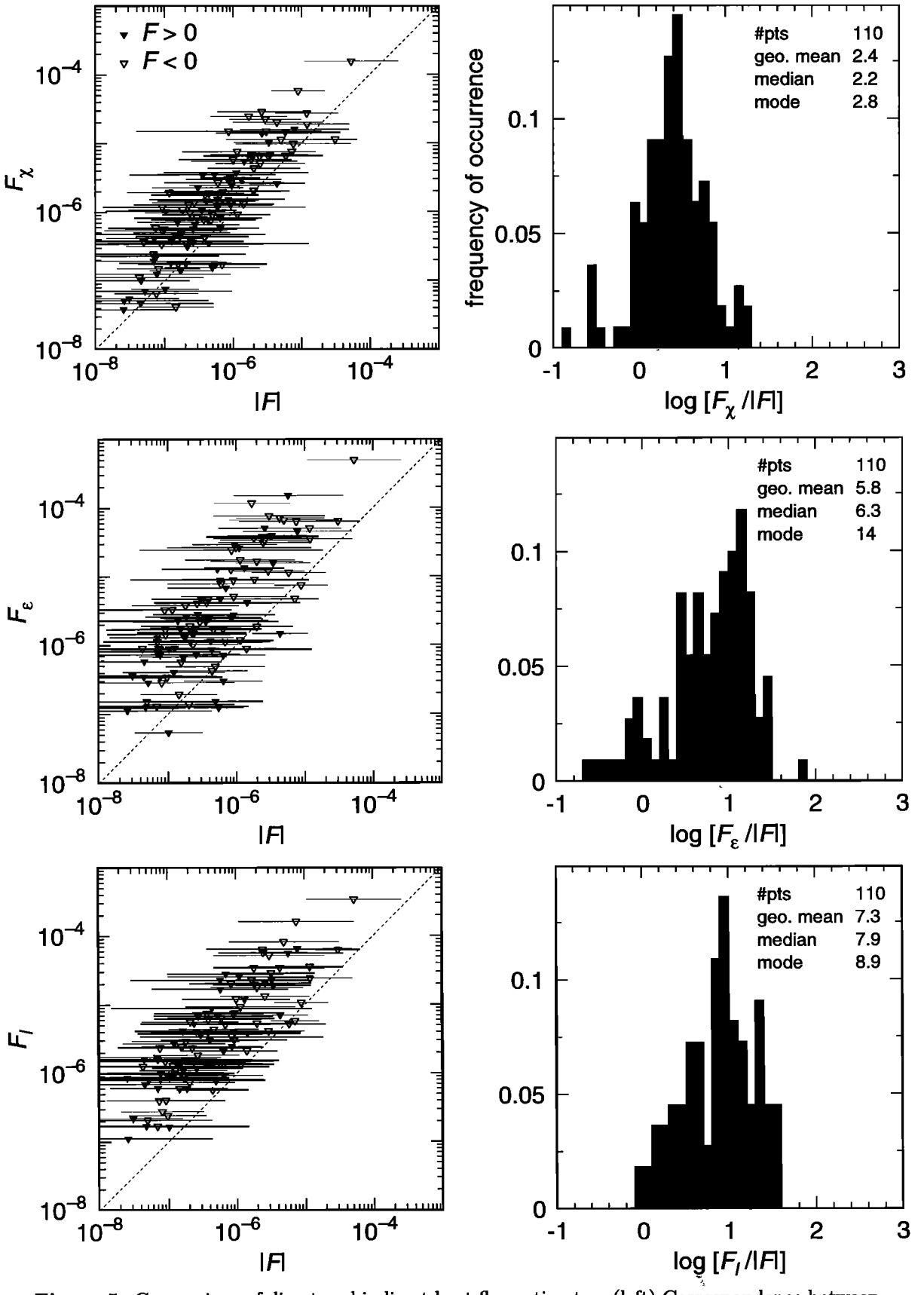

Figure 5. Comparison of direct and indirect heat flux estimates. (left) Correspondence between each of the pairs. (right) Histograms of the logarithms of ratios of ordinate to abscissa, together with measures of central tendency. Open triangles represent $F < 0$ (downgradient heat transport); solid triangles represent $F > 0$ (countergradient heat transport). Confidence intervals presented for F were computed using the estimates described in the text and shown in Figure 4.

ued into more energetic flow fields, such as the upper equatorial shear flows or the tidal fronts where patch thicknesses are greater and therefore record lengths are longer. However, these flows are not very amenable to this type of measurement since the energetic length scales become large compared to the body length, a factor which prohibits adequate resolution of the vertical

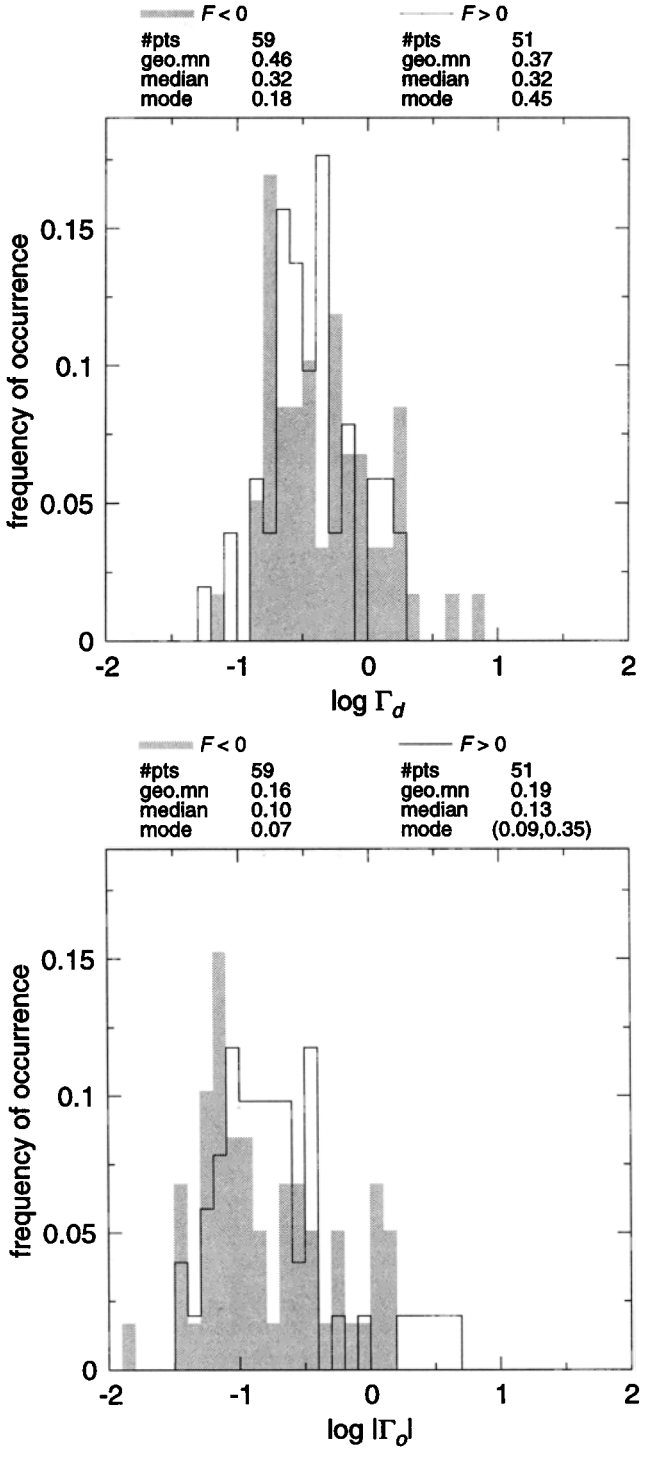

Figure 6. Histograms of the logarithm of dissipation flux coefficients, (top) $\Gamma_d = F_\chi/F_\epsilon$ and (bottom) $|\Gamma_o| = |F|/F_\epsilon$. The solid line represents $F > 0$, while the shaded area represents $F < 0$.

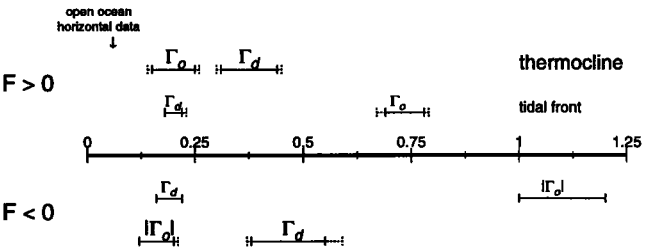

Figure 7. Ranges of 95% confidence intervals of the geometric mean values of the distributions of Γ_d, Γ_o shown in Figure 6. These were estimated by the bootstrap method (solid lines) and assuming normal statistics (dashed lines). The data discussed in this paper are represented by the large type, and the tidal front results discussed by *Gargett and Moum* [1995] are represented by the smaller type.

velocity spectrum at energy-containing scales, as discussed above. To make a meaningful comparison of direct and indirect flux estimates requires that the range of flux estimates be many times larger than the confidence in single estimates.

4. Dissipation Flux Coefficients

The comparison of direct and indirect flux estimates is represented by the scatterplots in Figure 5. The range of F is about 4 factors of 10 or many times the uncertainty in single estimates of F. The cloud of points outlined by the confidence limits of F indicate general agreement with all three indirect flux estimates, F_χ, F_ϵ, and F_ℓ (the mixing length estimate, $F_\ell \equiv w\ell T_z$, is defined by [*Moum*, 1996] and plotted here for completeness). The variability of the ratios of indirect to direct flux estimates is represented by the histograms in Figure 5 (right).

Histograms of $|\Gamma_o|$, Γ_d are shown in Figure 6. The ranges of estimates of Γ_d and Γ_o are shown in Figure 7, together with the estimates of GM95 from the turbulent tidal front. From Figures 6 and 7, the following several points are clear: (1) $\Gamma_d > |\Gamma_o|$; (2) the values of Γ_d, $|\Gamma_o|$ are independent of the sign of F; (3) estimates of Γ_d are within the range of open ocean observations of Γ_d [*Moum*, 1990a]; (4) estimates of $|\Gamma_o|$ are also within the range of open ocean observations of Γ_d; and (5) while thermocline estimates of Γ_d are significantly greater than those from the tidal front, thermocline estimates of $|\Gamma_o|$ are many times less than the tidal front estimates.

5. Discussion

The estimate of Γ_d ($\simeq 0.3 - 0.4$) for these thermocline data is on the high side of reported estimates from open ocean sites. Sample distributions of Γ_d from the thermocline data overlap those from the tidal front data. The large spreads in the distributions are likely due to combined measurement and sampling uncertain-

ties but may also reflect physical differences in the flow fields. Further discussion is based on measures of central tendency. These measures all indicate that the thermocline estimate of Γ_d is significantly greater than that from the tidal front. This might occur if the thermocline estimates of F_χ are biased high or F_ϵ biased low relative to other data sets. It is not clear how this could be since identical instrumentation, processing, and even some of the identical sensors were used in both thermocline and tidal front experiments to determine ϵ, χ, T_z, and N^2 which contribute to the estimates F_ϵ and F_χ. In particular, the computation of T_z may cause the estimates of F_χ (and hence Γ_d) to be biased high (section 2). Again, the same procedures were followed in both thermocline and tidal front experiments, so this cannot explain the differences in Γ_d between data sets.

The biggest difference between the two experiments is in the samples used to determine averaged values of indirect fluxes. For the thermocline data, independent samples have variable length and consist of single vertical profiles through turbulent patches with well-defined upper and lower boundaries. Although it is conceivable that a patch might be sampled more than once by subsequent profiles, the separation in both time and space between profiles is sufficiently great that no association of a particular patch with its previous history can be made with any certainty. In the case of the tidal front experiment (GM95) the flow field was almost completely turbulent. Using the horizontal measurements for guidance, regions of the flow which were reasonably homogeneous and/or stationary could be identified. All of the estimates of F_ϵ, F_χ (of which there may have been 100–200) within those regions were then treated as independent samples and averaged. Although we might expect greater uncertainty in estimates of mean values of F_ϵ, F_χ for the thermocline simply due to less well resolved natural variability, there is no reason to expect different mean values of Γ_d due simply to the sampling.

While these thermocline estimates of Γ_o ($\simeq$ 0.15 – 0.2) are within the range of open ocean estimates of Γ_d, they are significantly larger than the oceanic estimates of $\Gamma_o(\simeq$ 0.05) reported by YO93 and FL95. GM95 have suggested several reasons why each of these may be biased low. In particular, FL95 were able to clearly show that their estimates were limited by contamination of the low-wavenumber measurement of w by vehicle motion in cases where L_o^{-1} lies within the contaminated range of scales. In the cases where L_o^{-1} was smaller than this range of scales, their estimates indicate $\Gamma_o \simeq \Gamma_d \simeq 0.1$. The thermocline data chosen for analysis here have been carefully selected to exclude such occurrences (section 3).

The thermocline data were conditionally sampled in another manner. By invoking a test for significance of F estimates, similar to that used by YO93 and GM95, most of the smallest values of $|\Gamma_o|$ have been excluded from the analysis. From an original sample size of 272 this test reduced the number of samples to 110. Corresponding estimates of Γ_d were identical between the original and conditional samples. However, the estimate of $|\Gamma_o|$ for the original data set was 0.06 – 0.07 for both $F < 0$ and $F > 0$, compared with a value much closer to 0.2 from the conditionally sampled data shown in Figures 5 and 6. If the rationale for this means of conditionally sampling the data is valid, we must consider the higher value of $|\Gamma_o|$ to be the better estimate.

In direct contrast to the tidal front results, the thermocline data indicate $\Gamma_d > \Gamma_o$. Before examining the physical meaning of such a relationship, we must first consider whether Γ_d is biased high and/or Γ_o biased low relative to the other. From (4) and (5),

$$\frac{\Gamma_d}{\Gamma_o} = \frac{F_\chi}{F}. \tag{7}$$

As has already been indicated, the same procedure was used for the computation of F_χ for both thermocline and tidal front data sets. If F_χ is biased high from the thermocline measurements, then we must expect the same to be true for the tidal front estimates, and the difference between Γ_d and Γ_o to be greater than reported by GM95 (where $\Gamma_d > \Gamma_o$).

The other possibility is that the estimate of F obtained from vertical profiles in the thermocline is biased low. As noted, the conditional sampling for significance of F should tend to provide a high bias to F. Incomplete resolution of the space/time variability of the flux will produce a bias of unknown sign but should also apply to the estimates of F_χ and F_ϵ. Incomplete resolution of the flux cospectrum may produce a low bias, if the unresolved flux is associated with $F < 0$. However, this estimate of Γ_o is actually significantly greater than other reported oceanic estimates.

GM95 compared Γ_o and Γ_d via a reduced evolution equation for scalar variance, in which the time rate of change of available potential energy,

$$\eta = \frac{1}{2}\overline{\left(\frac{\rho'}{\rho_o}\right)^2}\left(\frac{g}{N}\right)^2, \tag{8}$$

is balanced by the buoyancy production of η and dissipation of η. That is,

$$\eta_t = b - \chi_\eta, \tag{9}$$

where χ_η is the dissipation rate of η (see GM95, equations (14) and (18)). GM95 also showed that $\Gamma_d = \chi_\eta/\epsilon$, so that, with $\Gamma_o = b/\epsilon$,

$$\Gamma_d = \frac{\chi_\eta}{\epsilon} = \frac{b - \eta_t}{\epsilon} = \Gamma_o - \frac{\eta_t}{\epsilon}. \tag{10}$$

GM95 argue that the tidal front may represent an example in which $\Gamma_d \leq |\Gamma_o|$. This will occur provided the time rate of change of available potential energy η_t has the same sign as the buoyancy flux b. A self-consistent scenario was suggested by GM95 for the case of the flow field produced by a tidal front. However, the more gen-

eral case may actually be $\Gamma_d > |\Gamma_o|$. Suppose that b is a sink for TKE (as it must be, on average, in a stratified fluid). Then, it is a source of η and $b > 0$. For a decaying turbulence, $\eta_t < 0$ and therefore $\Gamma_d > |\Gamma_o|$. The case represented by $b < 0$ is less straightforward but also of dubious importance in the continually stratified thermocline.

6. Summary and Conclusions

Estimates of heat flux by direct measurements of vertical velocity–temperature fluctuation correlations have been made from vertical profiles through turbulent patches in the main thermocline. These have been compared to more indirect flux estimates derived from dissipation rates of TKE and temperature variance.

Because the vertical dimension of turbulent patches in stratified fluids is presumed to be the small spatial dimension, vertical record lengths are correspondingly smaller than horizontal record lengths. As a consequence, the uncertainties cited here for individual estimates of F are considerably larger than would be obtained from horizontal measurements of F. These two estimates differ in another fundamental way. Temperature fluctuations are generally defined from high-pass-filtered representations of temperature records from horizontal measurements. An analogous representation from vertical profiles seems untenable, as sharp vertical gradients can appear as two-sided temperature fluctuations after filtering. So our basic definition of T' differs for vertical profile data. The difference between in situ and reordered temperature seems appropriate and is a one-dimensional analogue of the three-dimensional reordering used by *Winters et al.* [1995].

The flux-carrying scales are at least $O(10$ cm), confirming the preliminary results of *Moum* [1990a] and many times greater than the scales which dominate the dissipation rates of TKE and temperature variance. This is also many times less than the patch thickness.

Both Γ_d and Γ_o are within the range of open ocean estimates of Γ_d and laboratory estimates of Γ_o. They are very different from the values obtained in the turbulent tidal front by GM95. The range of values of both $|\Gamma_o|$ and Γ_d may be due either to unresolved variability of measured parameters within three-dimensional and evolving, turbulent patches or possibly due to different forms of instability leading to the observed turbulence (as suggested by GM95). However, it is impossible to tell what the cause of the variability is from these data. This will continue to be the case until we are able to make more complete observations of stratified turbulence in geophysical fluids and can clearly identify instability mechanisms.

If we consider measures of central tendency to adequately represent the true value of Γ_o, the present results suggest no obvious revision of dissipation flux estimates made in the ocean's thermocline based on a constant value $\Gamma_o = 0.2$. This implies a mixing efficiency or flux Richardson number of 0.17, in keeping with the original suggestion by *Osborn* [1980]. However, distributions of Γ_o (and Γ_d, for that matter) are consistently characterized by a large range of sample values (more than a factor of 10); this may be due to combined measurement and sampling uncertainties but may also indicate different physics at play. Consequently, and because of the very different result obtained from the tidal front by GM95, we should exercise considerable caution in extending this value of Γ_o to other flow fields. These may include mixed layers, boundary layers and flow fields dominated by energetic internal gravity waves in which advective instabilities are primarily responsible for turbulence generation.

The observation that $\Gamma_d > \Gamma_o$ may be the general case for stratified turbulence is in contrast to the tidal front result reported by GM95, which may represent an instructive but special case.

Acknowledgments. I have benefited considerably from many discussions with Ann Gargett. I thank Doug Caldwell for critical comments on an early draft. These data result from a group effort, notably the efforts of Mike Neeley-Brown, Ray Kreth, and Ed Llewellyn, in addition to Dave Hebert, who participated in the experiment and other aspects of the analysis. Many thanks to the students who helped at sea: Ayal Anis, Donna Witter, and Ed Zaron and to Pat Collier and Mylrea Estell. This work was funded by the Office of Naval Research (grant N00014-89-J-3211).

References

Dillon, T. M., Vertical overturns: A comparison of Thorpe and Ozmidov scales, *J. Geophys. Res.*, *87*, 541–549, 1982.

Fairall, C .W., J. B. Edson, S. E. Larsen, and P. G. Mestayer, Inertial-dissipation air-sea flux measurements: A prototype system using realtime spectral computations, *J. Atmos. Oceanic Technol.*, *7*, 425–453, 1990.

Fleury, M., and R. G. Lueck, Direct heat flux esimates using a towed body, *J. Phys. Oceanogr.*, *24*, 801–818, 1994.

Gargett, A. E., and J. N. Moum, Mixing efficiencies in turbulent tidal fronts: Results from direct and indirect measurements of density flux, *J. Phys. Oceanogr.*, *25*, 2583–2608, 1995.

Gregg, M. C., Diapycnal mixing in the thermocline: A review, *J. Geophys. Res.*, *92*, 5249–5286, 1987.

Hebert, D., and J. N. Moum, Decay of a near-inertial wave, *J. Phys. Oceanogr.*, *24*, 2334–2351, 1994.

Hebert, D., J. N. Moum, C. A. Paulson, and D. R. Caldwell, Turbulence and internal waves at the equator, II, Details of a single event, *J. Phys. Oceanogr.*, *22*, 1346–1356, 1992.

Huq, P., and R. E. Britter, Turbulence evolution and mixing in a two-layer stably stratified profile, *J. Fluid Mech.*, *285*, 41–68, 1995.

Kaimal, J. C., J. C. Wyngaard, Y. Izumi, and O.R. Cote, Spectral characteristics of surface layer turbulence, *Q. J. R. Meteorol. Soc.*, *98*, 563–589, 1972.

Lenschow, D. H., J. Mann, and L. Kristensen, How long is long enough when measuring fluxes and other turbulence statistics?, *J. Atmos. Oceanic Technol.*, *11*, 661–673, 1994.

Moum, J. N., The quest for K_ρ - Preliminary results from direct measurements of turbulent fluxes in the ocean, *J. Phys. Oceanogr.*, *20*, 1980–1984, 1990a.

Moum, J. N., Profiler measurements of vertical velocity microstructure in the ocean, *J. Atmos. Oceanic Technol.*, *7*, 323–333, 1990b.

Moum, J. N., Energy-containing scales of stratified turbulence in the ocean thermocline, *J. Geophys. Res.*, in press, 1996.

Moum, J. N., M. C. Gregg, R-C. Lien, and M-E. Carr, Comparison of turbulent kinetic energy dissipation rate estimates from two ocean microstructure profilers, *J. Atmos. Oceanic Technol.*, *12*, 346–366, 1995.

Osborn, T. R., Estimates of the local rate of vertical diffusion from dissipation measurements, *J. Phys. Oceanogr.*, *10*, 83–89, 1980.

Osborn, T. R., and C. S. Cox, Oceanic fine structure, *Geophys. Fluid Dyn.*, *3*, 321–345, 1972.

Peters, H., M. C. Gregg, and T. B. Sanford, Detail and scaling of turbulent overturns in the Pacific Equatorial Undercurrent, *J. Geophys. Res.*, *100*, 18,349–18,368, 1995.

Pond, S., J. E. Paquin, G. McBean, and R. W. Stewart, Measurements of the turbulent fluxes of momentum, moisture and sensible heat over the ocean, *J. Atmos. Sci.*, *28*, 901–917, 1971.

Rohr, J., and C. Van Atta, Mixing efficiencies in stably stratified growing turbulence, *J. Geophys. Res.*, *92*, 5481–5488, 1987.

Thorpe, S. A., Turbulence and mixing in a Scottish loch, *Philos. Trans. R. Soc. London A*, *286*, 125–181, 1977.

Winters, K. B., P. N. Lombard, J. J. Riley, and E. A. D'Asaro, Potential energy and mixing in density stratified flows, *J. Fluid Mech.*, *289*, 115–128, 1995.

Yamazaki, H., and T. R. Osborn, Direct estimation of heat flux in the seasonal thermocline, *J. Phys. Oceanogr.*, *23*, 503–516, 1993.

J. N. Moum, College of Oceanic and Atmospheric Sciences, Oregon State University, 104 Ocean Admin Building, Corvallis, OR 97331-5503. (e-mail: moum@oce.orst.edu)

(Received August 4, 1995; revised January 9, 1996; accepted January 15, 1996.)